



Annualized exergoenvironmental comparison of solar-only and hybrid solar-biomass heat interactions with an organic Rankine cycle power plant

Joseph Oyekale^{a,*}, Mario Petrollese^b, Daniele Cocco^b, Giorgio Cau^b

^a Department of Mechanical Engineering, Federal University of Petroleum Resources Effurun, P.M.B. 1221 Effurun, Delta State, Nigeria

^b Department of Mechanical, Chemical and Materials Engineering, University of Cagliari, Via Marengo 2, 09123 Cagliari, Italy

ARTICLE INFO

Keywords:

Organic Rankine Cycle
Exergoenvironmental Analysis
Renewable Power Plant
Hybrid Solar-Biomass Plant

ABSTRACT

This study is aimed at comparing the environmental performance of a solar-only and hybrid solar-biomass organic Rankine cycle (ORC) plant using the exergoenvironmental method. The system studied adopts the design features of a real ORC plant currently running at Ottana, Italy, rated nominally at about 630 kW. Established procedures of the exergoenvironmental methods were applied, which integrate the principles of exergy and life cycle analyses. The method quantifies the yearly environmental impact rates of each of the plant components. The eco indicator-99 impact assessment method was adopted to quantify impact rates. Results showed that implementing the biomass hybridization scheme would improve the annualized exergetic efficiency of the existing solar ORC plant by about 3 percentage points, from about 7% with solar-only to about 10% with hybrid solar-biomass heat sources, although a small increase in the relative irreversibility rate is observed (from 49% to 51%). It would as well improve the capacity factor of the plant. However, the environmental impacts would be impacted negatively. Particularly, the specific exergoenvironmental impact rates were obtained as 27.4 Pts/MWh for the hybrid solar-biomass ORC plant, as against 20.3 Pts/MWh obtained for the solar-only plant, implying that the hybridization strategy would increase impact rate by about 35%. Similarly, it was obtained that biomass hybridization would increase the overall exergoenvironmental impact rates of the ORC plant by about 92,000 Pts/year, due majorly to increased exergy destruction in the plant components and the polluting emissions of the combustor.

Introduction

A steep rise in the global population today leads to a significant increase in energy demand [1]. Thus, to satisfy demands, energy generation systems are being expanded substantially, most of which still use fossil fuels as primary sources [2]. However, the conventional energy systems running on fossil fuels generally threaten the sustainability of man and the ecosystem due to hazardous gaseous emissions. Consequently, intense research and technical efforts are underway to develop energy systems that would run on renewable and clean fuels. The main renewable energy sources in focus include solar energy, wind energy, biomass energy, geothermal energy, etc. Specifically, energy production from solar irradiation is currently being vigorously explored globally, perhaps because the sun shines everywhere, free of charge. In particular, concentrating solar power (CSP) is an effective technology for the conversion of solar energy into electricity. Nevertheless, these systems are characterized by low capacity factors and high costs of power

production, due majorly to the transient availability of solar irradiation. To mitigate these effects, CSP systems are usually integrated with thermal energy storage devices. However, in CSP plants thermal energy production can also be integrated by other and more dispatchable renewable sources, such as biomass and geothermal energy [3]. The fact that biomass fuels are more readily and spatially available than geothermal wells has brought hybrid solar-biomass energy systems to the spotlight.

Research focus on hybrid solar-biomass energy systems is diverse, including conceptual and detailed design, modeling and simulation, optimization, etc. Research interests often lie between the development of new energy systems and the improvement of existing fully-solar or fully-biomass plants through retrofit. As mentioned above, a lot of research attention is currently being given to this theme; a few of the most recent articles available in the literature are highlighted here. Middelhoff *et al.* [4] carried out a comprehensive study to investigate the feasibility of a hybrid solar-biomass steam power plant in Australia. The study adopted CSP system and biomass boiler using rice husk as the

* Corresponding author.

E-mail address: oyekale.oyetola@fupre.edu.ng (J. Oyekale).

Nomenclature		Δh	enthalpy change (kJ/kg)
Symbols		ρ	mass density (kg/m ³)
b	specific exergoenvironmental impact (Pts/MWh)	η	exergetic efficiency
\dot{B}_I	exergoenvironmental impact rate due to irreversibility (Pts/year)	Subscripts	
EIE	exergoenvironmental impact per unit energy produced (Pts/MWh)	A	annual
\dot{E}	rate of exergy (kW)	a	ambient
e	specific exergy (kJ/kg)	biom	biomass
f_b	exergoenvironmental factor	c	component boundary
h	enthalpy (kJ/kg)	cond	condenser
\dot{I}	rate of destroyed exergy/irreversibility (kW)	eff	effective
LHV	lower heating value (MJ/kg)	F	fuel
\dot{m}	mass flow rate (kg/s)	i	inlet side
N	plant lifetime (years)	k	component identifier
Q	thermal energy (kWh)	l	liquid
\dot{Q}	thermal power (kW)	o	outlet side
\dot{q}	heat flux (W/m ²)	P	product
\dot{R}	total exergoenvironmental impact rate	pm	pump motor
RI	relative irreversibility	sk	sink
r_b	specific exergoenvironmental impact rate difference	Superscripts	
s	specific entropy (kJ/kgK)	PF	<i>pollutant formation</i>
T	temperature (°C)	Abbreviations	
\dot{W}	electrical power (kW)	CSP	concentrating solar power
\dot{Y}	exergoenvironmental impact rate due to component construction/pollutant emission (Pts/year)	HTF	heat transfer fluid
Greek letters		LCA	life cycle assessment
ΔT	temperature change (K)	LFC	linear Fresnel collector
		ORC	organic Rankine cycle
		TES	thermal energy storage

combustible fuel. The authors reported that efficiency of between 21% and 34% would be obtainable with plant nominal size varying from 5 MW to 50 MW. Moreover, the study highlighted that substantial techno-economic gain was obtainable using the hybrid solar-biomass design, compared to stand-alone solar or biomass systems. Similarly, Tilahun *et al.* [5], in their optimal design study for the use of a hybrid solar-biomass system to satisfy industrial energy needs, obtained that thermal efficiency of about 32% was possible with a corresponding leveled cost of energy of 0.13 \$/kWh. Nami *et al.* [6] proposed a hybrid solar-biomass system for cogeneration of 1 MW of electrical power, about 1343 kW of thermal energy (for space heating and hot water production), and about 55 kW of chilled water. Applying exergy-based methods to investigate performance, the study concluded that the proposed hybrid system could satisfy domestic energy needs sustainably. Also, Pina *et al.* [7] analyzed the thermo-economic performance of an organic Rankine cycle cogeneration plant using a hybrid solar-biomass heat source. The hybrid plant was designed to satisfy the electrical energy and cooling needs of a commercial data center in Spain. Following a comprehensive analysis, the authors reported that the plant needed substantial economic optimization to run profitably; although it could facilitate the reduction of CO₂ emissions.

While most of the literature review on hybrid solar-biomass plants hinted at the importance of environmental sustainability aspects, not so much has been done to incorporate into the analysis, detailed environmental considerations over the entire life cycle. A popular method being employed nowadays for assessing the environmental feasibility of sustainable energy plants is the exergoenvironmental analysis, achieved as an offshoot of the exergy method by including the life cycle analysis (LCA) methodology. It was first proposed by Meyer *et al.* [8] in the year 2009. Since then, the exergoenvironmental method has been applied to analyze different types of energy systems, especially during feasibility

studies of newly proposed plants based on renewable energy. Cavalcanti *et al.* [9] investigated the exergoenvironmental performance of a renewable cogeneration plant in Brazil that uses sugarcane bagasse as fuel. Adopting the eco indicator-99 method for LCA, the study reported about 6 mPt/MJ specific exergoenvironmental impact for the plant, which was reportedly better than what obtains in more conventional systems running on fossil fuels. Mohammadi Hadelu and Ahmadi Boyaghchi [10] employed the exergoenvironmental method to compare four solar-fuelled expander-organic flash cycle plants, reporting that the approach contributed substantially to the design process. Aghbashlo *et al.* [11] assessed the exergoenvironmental performance of a cogeneration plant producing power and fertilizer from organic municipal solid wastes. Environmental impacts of all the plant components were reported and the study proposed recommendations on how to improve performance metrics. Wang *et al.* [12] proposed and studied the exergoenvironmental performance of an ORC plant generating electrical power and useful heat from geothermal water. The study reported that very low exergy-based environmental impact was achievable with adequate optimization of the plant operation. Bonforte *et al.* [13] equally employed the exergoenvironmental method to quantify the reduction in environmental impact that could be obtained by hybridizing a gas power plant with a solar energy system. The authors reported that such hybridization would reduce environmental impact significantly, albeit at a higher investment cost. Additionally, the exergoenvironmental method is being applied in the literature to study the impacts of green generation of hydrogen and other renewable fuels [14,15,16,17,18,19].

It is explicit from the foregoing that exergoenvironmental assessment has gradually become an important method; it is considered essential for the complete analysis of new energy technologies. Although it has been applied widely to assess diverse renewable energy systems, no

exergoenvironmental results are found in the literature for hybrid solar-biomass systems, to the authors' best knowledge. Also, most published studies on exergoenvironmental assessment of solar energy systems reported results at design points, which may not represent the true performance throughout the year, due to the transient nature of solar energy. These lacks constitute potent research gaps, given the popularity of solar-based systems as mentioned earlier.

This paper aims to present for the first time results of annualized exergoenvironmental analysis of a hybrid solar-biomass organic Rankine cycle plant. The hybrid plant analyzed is based on a real 630 kW ORC plant currently running at Ottana, Italy. It is currently powered by linear Fresnel concentrating collectors, and studies are in progress to assess the feasibility of parallel hybridization of a biomass system. Previous studies on the power plant have demonstrated the potential techno-economic benefits of introducing biomass hybridization [20,21], also based on the Second Law of Thermodynamics [22]. However, the expected negative impacts that such hybridization would have on the environment remain unaccounted, thereby necessitating the current study. The specific objectives of the current paper are:

- To compare yearly exergetic performance of components and overall systems for the solar-only and hybrid solar-biomass ORC plants;
- To quantify environmental impact of the proposed hybrid solar-biomass ORC plant using established exergoenvironmental procedures, and compare performance with that of the current solar-only system;
- To evaluate the contribution of each system component to the total environmental impact rate of the hybrid plant;
- To examine the main source of exergoenvironmental impact rate - thermodynamic irreversibility in components during operation, or component construction processes/pollutant emissions.

Section two of this article describes in detail the layout of the hybrid plant as well as the procedures for the exergoenvironmental methods applied. The exergoenvironmental results are reported and compared in section three, for the solar-only and hybrid solar-biomass plants; while the main conclusions are summarised in section four.

Methodology

Description of plant layout and design features

The hybrid solar-biomass plant that is the focus of this study is

illustrated in Fig. 1. It has four main sub-units: the solar field (SF) unit, the thermal energy storage (TES) unit, the biomass unit, and the organic Rankine cycle (ORC) unit. The SF unit comprises six collector lines based on the Linear Fresnel collector technology. It utilizes a thermal oil (Therminol SP-I) as the heat transfer fluid (HTF) in the receiver to absorb useful thermal energy from the sun. The SF unit is linked directly to the TES system; the heated thermal oil leaving the SF flows into the TES hot tank (HT) and, after utilizing the stored energy during the discharge process, it accumulates in the cold tank (CT), from where it flows into the SF unit for recirculation. The biomass unit comprises mainly of a combustion chamber, where solid (woody) biomass is burnt for heat generation, and a heat exchanger, which is often referred to as the furnace heater. The hot combustion gases leaving the combustion chamber exchange heat in the furnace heater with a heat carrier, the same thermal oil (Therminol SP-I), as shown in Fig. 1. The biomass fuel adopted in this study is the Sardinian eucalyptus, with the main features after a natural drying highlighted in Table 1 [23], due to its availability at the site of the power plant. The ORC unit is a 630-kW module designed and built by Turboden, known technically as Turboden 6HR Special. The unit is a regenerative power plant using an organic fluid, hexamethylidisiloxane (MM), as the working medium. The heat source, hot thermal oil flowing from the SF via the TES hot tank, elevates the thermal content of the ORC working fluid in a pre-heater, before evaporating same in the evaporator. The evaporated MM is then expanded through a turbo-generator for electrical power production. The expanded ORC working fluid is condensed back to liquid using water as a heat sink in the condenser. Then, the pressure of the working fluid is raised through the pump, while a part of the waste heat of the working fluid at the turbine exit is recovered (recuperated) and used internally to pre-heat the same working fluid. In the case where only solar energy is considered as the heat source for the plant, the entire biomass unit is bypassed from Fig. 1, and all other system characteristics remain the same. The main design features of all the hybrid plant sub-units are also highlighted in Table 1, based on the real solar-ORC plant that currently runs at Ottana (Italy).

Annual simulation

Simulation of the annual performance of the solar-biomass plant required dedicated modelling of the entire plant and therefore, previously developed models were applied in this study. The models, implemented in Matlab, permitted the evaluation of the inlet/exit flows of mass, enthalpy, heat, and work for each system component, at

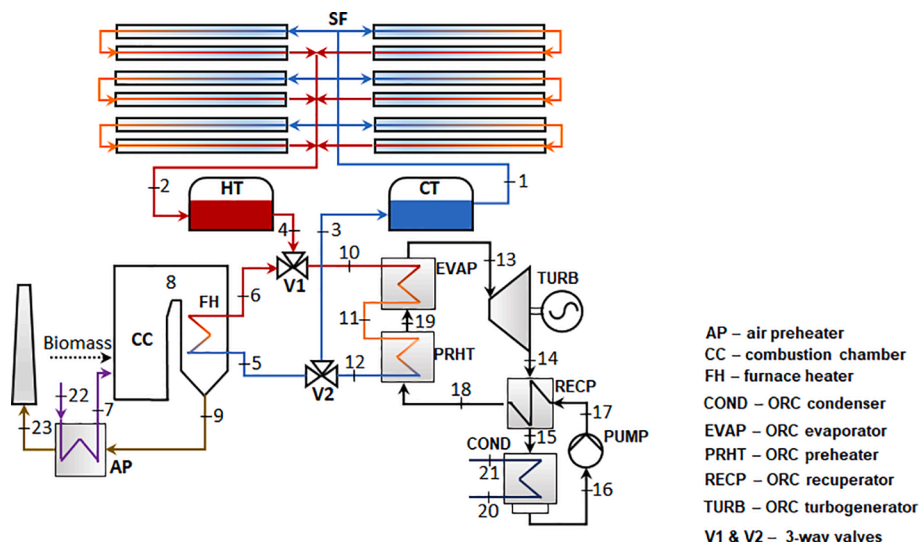


Fig. 1. Conceptual scheme for the hybrid CSP-biomass ORC plant [20].

Table 1
Design features of the ORC plant with hybrid CSP-biomass heat source [20].

Solar Field		ORC unit	
Focal length of the collector	4.97 m	Working fluid	C ₆ H ₁₈ OSi ₂
Length of collector	99.45 m	Heat sink	Water
Solar field net area	8400 m ²	Net electrical power	0.629 MW
Optical efficiency	0.64	Nominal input thermal power	3.178 MW
Average air temperature	298 K	Nominal HTF flow rate	11.05 kg/s
Average air pressure	1 atm	Isentropic efficiency - pump	0.80
Nominal inlet temperature	438 K	Motor efficiency - pump	0.98
Nominal exit temperature	548 K	Isentropic efficiency - turbine	0.85
Nominal thermal losses	3%	Electromechanical efficiency	0.92
TES system		Biomass Combustion	
Storage capacity	15.4 MWh	Furnace thermal duty	1.430 MW
Tank useful volume	330 m ³	Fuel composition (dry basis, % by weight)	48.3 % C, 5.9 % H, 0.1 % N ₂ , 38.5 % O ₂ , 7.2 % Ash
Aspect ratio	0.32		
Ambient wind speed	3 m/s		
Insulation thickness	0.5 m	LHV (dry basis)	16.3 MJ/kg
Insulation thermal conductivity	0.16 W/m ² K	Moisture content	20 %
		Stoichiometric air-fuel ratio	5
		Excess air	150 %
		Combustion efficiency	99 %

intervals of 1 h. Specifically, starting from the expected annual weather data for the Ottana site provided by Meteonorm software [24], the model proposed in [25] was adopted for the evaluation of the performance of the solar field and the TES section, while the model proposed in [20] was used for the simulation of the biomass furnace. The annual direct normal irradiance (DNI) availability at the Ottana site of the power plant was estimated at about 1.74 MWh/(m².year) based on the data from the Meteonorm software. The HTF mass flow rate heated up by the furnace was arranged to keep an outlet HTF temperature constant. The biomass required to supply the hourly thermal duty required was then assessed. The thermal production of the solar field and the biomass furnace are mixed in the valve V1, consequently, the management of this valve determines the operability of the ORC unit. In this work, it is assumed that the biomass furnace works continuously (8760/year) by supplying 45% of the nominal thermal power input required by ORC; the design assumption is premised on the results reported in [20] and it assures the operation of the plant at its minimum part load. The thermal power produced by the solar field is stored in the hot tank until the 60% of the nominal storage capacity of the hot tank is reached. When these conditions are satisfied, the solar thermal energy contributes to the supply to the ORC, which is fed by a HTF mass flow rate equal to the nominal one. The ORC unit will be supplied by a nominal HTF mass flow rate until the state-of-charge of the hot tank drops below 20%. Finally, the performance of the ORC unit is evaluated according to the models proposed in [26], which are experimentally validated using off-design operational data from the referenced ORC plant at Ottana. Starting from the HTF mass flow rate feeding the ORC and the corresponding temperature, as well as the cooling inlet temperature (directly connected to the ambient temperature), the net power produced by the ORC and the HTF outlet temperature are calculated.

Exergoenvironmental assessment of the hybrid plant

The exergoenvironmental analysis carried out in this study combines exergy and life cycle assessments (LCA), to investigate the impacts of the system components on the environment. Firstly, annualized exergy balances were established for the different components and sub-units, as expressed mathematically in Eq. (1):

$$\sum E_i + Q \left(1 - \frac{T_a}{T_c}\right) = \sum E_o + W + I \tag{1}$$

In the balance equations above E, Q, W, and I represent exergy, heat flow through the component, work done by the component and exergy destroyed (irreversibility), respectively, obtained and accumulated over 8760 points of plant operation in a year at 1-hour interval. The parameters T_a and T_c are respectively the ambient and component surface temperature, while the subscripts i and o indicate the inlet to, and exit from a component, respectively. Then, the net annualized exergy entering each of the system components (fuel exergy, E_f) and the net annualized exergy leaving (product exergy, E_p) were defined. Table 2 summarizes the annualized fuel and product exergy defined for all the main components of the hybrid solar-biomass ORC plant being reported.

The standard life cycle assessment approach was employed to characterize the environmental impacts of the hybrid plant. Conventional LCA comprises four main stages, used for investigating the impacts of a product or process on the environment over its entire life cycle [27]. In the first stage, the study goal and scope are defined, including specification of the boundary of analysis, selection of impact categories, and characterization factors. The second stage entails life cycle inventory analysis where all the material and energy flows in and out are estimated. In the third stage, impact assessments are carried out using suitable impact assessment methods often embedded in LCA software. Lastly, the results obtained in the previous stages are interpreted to examine the effects of the system on the environment.

However, in exergoenvironmental analysis, it is required to assign environmental impacts to each exergy stream for the components and the overall system. Thus, next to goal and scope definition and inventory analysis based on the system model, it is common to adopt a point-based environmental impact method for the exergy streams. In this study, the eco-indicator-99 (EI-99) impact identifier was adopted to assign environmental impact to component/system streams. The EI-99 method obtains a single environmental index for processes and products by weighting in hierarch perspective three main damage aspects: ecosystem quality, human health, and natural resources [28]. The method provides indices in millipoints (mPts) or points (Pts) for several processes and products based on the LCA international standards [8]. The higher the EI-99 points obtained for each exergy stream or system component, the higher the damage done by such process/component to the environment. After the environmental impacts in points have been assigned to system components/streams, the exergoenvironmental

Table 2
Fuel and product exergy for components.

Component (abbreviation)	Fuel exergy	Product exergy
Solar field (SF)	E _s	E ₂ - E ₁
Hot tank (HT)	E ₂	E ₄
Cold tank (CT)	E ₃	E ₁
Air preheater (AP)	E ₉ - E ₂₃	E ₇ - E ₂₂
Combustion chamber (CC)	E _b + E ₇	E ₈
Furnace heater (FH)	E ₈ - E ₉	E ₆ - E ₅
ORC preheater (PRHT)	E ₁₁ - E ₁₂	E ₁₉ - E ₁₈
Evaporator (EVAP)	E ₁₀ - E ₁₁	E ₁₃ - E ₁₉
Recuperator (RECP)	E ₁₄ - E ₁₅	E ₁₈ - E ₁₇
Condenser (COND)	E ₁₅ - E ₁₆	E ₂₁ - E ₂₀
Pump (PUMP)	W _{PUMP}	E ₁₇ - E ₁₆
Turbine (TURB)	E ₁₃ - E ₁₄	W _{TURB}
Valve 1 (V1)	E ₄ + E ₆	E ₁₀
Valve 2 (V2)	E ₁₂	E ₃ + E ₅

variables are calculated, for exergy-based LCA evaluation of the system.

Meyer *et al.* [8] who first applied the exergoenvironmental method, proposed an exergoenvironmental balance equation that is analogous to the cost balance equation in the exergoeconomic method. The balance equation at the component level, defined below in eqs. (2) and (3), has become the bedrock of the exergoenvironmental analysis today:

$$\sum B_i + B_q + (Y + B^{PF}) = \sum B_o + B_w \quad (2)$$

$$\sum b_i E_i + b_q Q + (Y + B^{PF}) = \sum b_o E_o + b_w W \quad (3)$$

where B is the environmental impact rate (over 1 year in this study), expressed as the product of the specific environmental impact of a stream (b , Pts/MWh) and annual exergy rate (E , MWh/year), subscripts i , o , q and w represent inlet flow to a component, exit flow from the component, the flow of heat to and the flow of work from the component, respectively, B^{PF} is the environmental impact rate due to pollutant formation in the component and Y is the environmental impact rate related to the component, obtained as a sum of impacts due to its construction, Y^{CO} , operation and maintenance, Y^{OM} and disposal, Y^{DI} . Also, B^{PF} for a component is given as:

$$B^{PF} = \sum_n b_n^{PF} (\dot{m}_{n,out} - \dot{m}_{n,in}) \quad (4)$$

where b_n^{PF} is the specific environmental impact due to emission of pollutant n from a component (Pts/kg), with mass flow rates $\dot{m}_{n,in}$ at the inlet of the component and $\dot{m}_{n,out}$ at the exit.

The annualized exergoenvironmental balance equations are defined in Table 3 for all the components of the hybrid plant. The component environmental impacts were computed in EI-99 points based on the material composition and weight of each component. The composition and weight of the hybrid plant components/sub-units were obtained from inventory analysis and considering manufacturer specifications for the respective plant units, using the ecoinvent database [29,30]. The specific quantitative values used in this study are tabulated in Appendix I. The environmental impact rates of the dissipative components (separating valves V1 & V2) were added to that of the productive component (turbine). Also, it was assumed that emission released directly to the environment (b_n^{PF}) is most prominent in the biomass combustion section. However, since carbon and its oxides are consumed for plant growth, the net direct emission from the combustion chamber was taken to be zero. Next, to obtain specific environmental impact (b) for each stream, the product-fuel (P-F) rule was applied to formulate auxiliary equations in addition to the environmental balance equations,

Table 3
Exergoenvironmental balance and auxiliary equations.

Component (abbreviation)	Exergoenvironmental rate balance equation	Auxiliary equation
Solar field (SF)	$B_1 + B_{sun} + Y_{SF} = B_2$	$b_{sun} = 0$
Hot tank (HT)	$B_2 + Y_{HT} = B_4$	
Cold tank (CT)	$B_3 + Y_{CT} = B_1$	
Air preheater (AP)	$B_{22} + B_9 + Y_{AP} = B_{23} + B_7$	$b_{22} = 0; b_9 = b_{23}$
Combustion chamber (CC)	$B_7 + B_{biom} + Y_{CC} = B_8$	$b_{biom} = 2.128 \frac{\text{Pts}}{\text{MWh}}$ [32]
Furnace heater (FH)	$B_8 + B_5 + Y_{FH} = B_9 + B_6$	$b_8 = b_9$
ORC preheater (PRHT)	$B_{11} + B_{18} + Y_{PRHT} = B_{19} + B_{12}$	$b_{11} = b_{12}$
Evaporator (EVAP)	$B_{10} + B_{19} + Y_{EVAP} = B_{11} + B_{13}$	$b_{10} = b_{11}$
Recuperator (RECP)	$B_{14} + B_{17} + Y_{RECP} = B_{15} + B_{18}$	$b_{14} = b_{15}$
Condenser (COND)	$B_{15} + B_{20} + Y_{COND} = B_{16} + B_{21}$	$b_{20} = 0; b_{15} = b_{16}$
Pump (PUMP)	$B_{16} + B_{w,p} + Y_{PUMP} = B_{17}$	$b_{w,p} = b_{w,t}$
Turbine (TURB)	$B_{13} + Y_{TURB} + Y_{V1} + Y_{V2} = B_{w,t} + B_{14}$	$b_{13} = b_{14}$
Valve 1 (V1)	$B_4 + B_6 = B_{10}$	$b_4 = b_6 = b_{10}$
Valve 2 (V2)	$B_{12} = B_3 + B_5$	$b_{12} = b_3 = b_5$

shown also in Table 3. The balance and auxiliary equations were then solved simultaneously for all components, in analogy to what is done to obtain the specific cost of a stream in the specific exergy costing (SPECOC) exergoeconomic approach [31].

Exergoenvironmental evaluation parameters

The main exergoenvironmental parameters used to evaluate the annual performance of each system component are: exergy efficiency (η_{ex}), relative irreversibility (RI), mean specific fuel exergoenvironmental impact (b_F), mean specific product exergoenvironmental impact (b_P), exergoenvironmental impact rate due to irreversibility in system component (B_I), total exergoenvironmental impact rate (R), exergoenvironmental factor (f_b), specific exergoenvironmental impact relative difference (r_b) and exergoenvironmental impact per unit energy produced (EIE). Again, all the parameters were accumulated for 8760 h, for annualized assessment. For a system component k , the aforementioned exergoenvironmental parameters are defined respectively as:

$$\eta_{ex,k} = \frac{E_{P,k}}{E_{F,k}} \quad (5)$$

$$RI_k = \frac{I_k}{\sum_{k=1}^z I_k} \quad (6)$$

$$b_{F,k} = \frac{B_{F,k}}{E_{F,k}} \quad (7)$$

$$b_{P,k} = \frac{B_{P,k}}{E_{P,k}} \quad (8)$$

$$B_{I,k} = b_{F,k} \times I_k \quad (9)$$

$$R_k = B_{I,k} + Y_k \quad (10)$$

$$f_{b,k} = \frac{Y_k}{B_{I,k} + Y_k} \quad (11)$$

$$r_{b,k} = \frac{b_{P,k} - b_{F,k}}{b_{F,k}} \quad (12)$$

$$EIE_k = \frac{R_k}{W_{net}} \quad (13)$$

The exergoenvironmental impact rates for fuel ($B_{F,k}$) and product ($B_{P,k}$) were obtained using the P-F rule after values for b have been obtained for all streams of the system. While the difference between exergy rate for fuel and product for a component k gives the irreversibility, I_k . The superscript ‘ z ’ in eq (6) is the total number of system components.

Results and discussion

Exergoenvironmental characteristics of the system thermodynamic states

The introduction of the biomass hybridization scheme led to an increase in the annual electrical energy produced by the plant from 0.70 GWh/year for the solar-only case to 3.20 GWh/year. Similarly, the capacity factor increased from about 1120 h/year for the solar-only plant to about 5080 h/year for the hybrid plant. A total of 4884 tonnes/year of woody biomass was consumed by the hybrid plant, and this is expected to have a negative impact on the environmental sustainability of the system.

The exergetic and environmental features of each state of the hybrid plant are highlighted in Table 4. To obtain the specific environmental impact (b) at each thermodynamic state, the set of exergoenvironmental balance and auxiliary equations reported in Table 3 were solved simultaneously, as aforementioned. And once b values were known, the environmental impact parameters became obtainable based on eqs (5)–

Table 4
Exergetic and environmental features of each state of the hybrid plant.

Stream ID	Working substance	Exergy (MWh/year)	b (Pts/MWh)	B(Pts/year)
1	Thermal oil	2037.1	7.256	14780.4
2	Thermal oil	2842.7	5.649	16058.6
3	Thermal oil	2098.4	6.886	14448.8
4	Thermal oil	2799.9	5.854	16390.1
5	Thermal oil	3387.7	6.886	23326.5
6	Thermal oil	10902.9	7.150	77960.9
7	Air	42.8	29.734	1272.4
8	Combustion gases	11665.2	5.058	59006.6
9	Combustion gases	864.4	5.058	4372.3
10	Thermal oil	13702.7	6.886	94351.1
11	Thermal oil	9220.1	6.886	63485.8
12	Thermal oil	4481.3	6.886	30856.3
13	MM	8201.2	12.428	101927.6
14	MM	2934.0	12.428	36464.8
15	MM	943.8	12.428	11729.7
16	MM	45.0	12.428	558.7
17	MM	111.8	26.295	2940.4
18	MM	1663.5	18.262	30378.9
19	MM	4964.3	13.176	65411.9
20	Water	0	0	0
21	Water	184.7	64.412	11894.6
22	Air	0	0	0
23	Combustion gases	619.0	5.058	3130.9

(13). The absolute values obtained for b and \dot{B} at each thermodynamic state are indispensable for the environmental analysis of each system component, discussed hereunder.

Exergetic comparison of the solar-only and hybrid solar-biomass plants

The annualized exergy efficiency and relative irreversibility are indicative of the technical performance of the solar-only and the hybrid plant components. It is desired that a system component should have high exergy efficiency and low relative irreversibility. Results in Fig. 2 and Fig. 3 show that the thermodynamic performance of the ORC plant is improved using the hybrid solar-biomass system. Specifically, the annualized exergy efficiency of the ORC plant is significantly improved (by about 3 percentage points) with the use of a hybrid solar-biomass heat source, relative to the solar-only alternative. However, except solar field and condenser, exergy efficiencies for system components for the two cases are fairly the same in all components, obviously due to closely-match ORC designs implemented. Moreover, it can be inferred

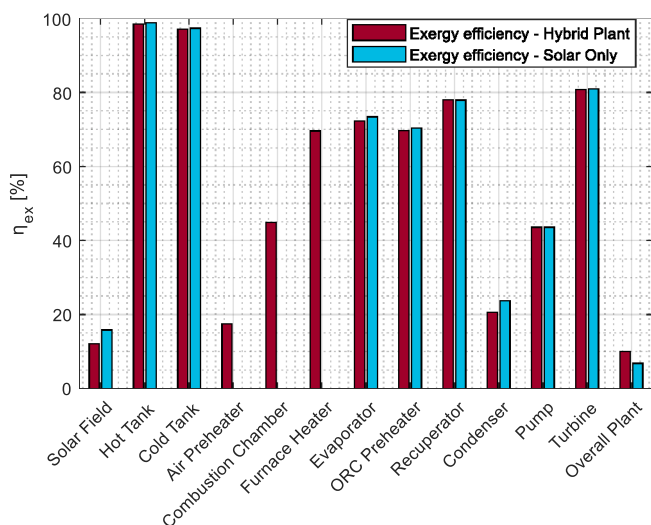


Fig. 2. Components and plant exergy efficiencies – hybrid vs. solar-only systems.

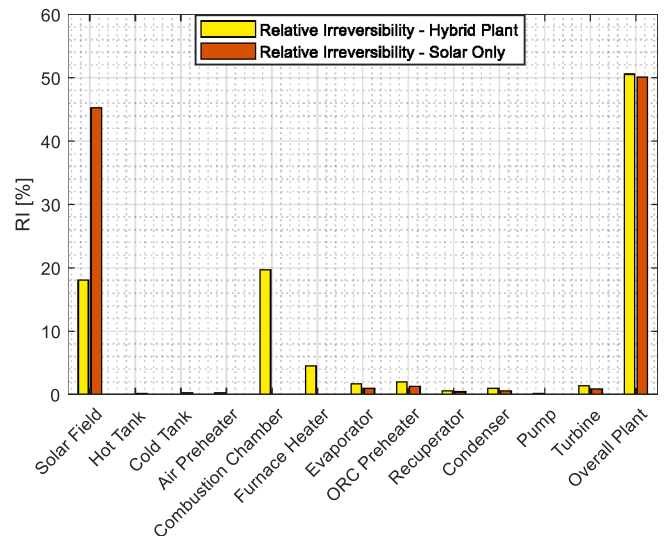


Fig. 3. Components and plant relative irreversibilities – hybrid vs. solar-only systems.

from Fig. 5 that adopting the hybrid solar-biomass heat source would reduce considerably the exergy losses in the solar field. Overall, adding the biomass energy input would lead to enhanced availability of the ORC to produce energy, thereby increasing the overall integrated power plant capacity factor.

Exergoenvironmental analysis results

Hybrid solar-biomass plant

Table 5 presents the exergoenvironmental impact results for the hybrid plant components. The highest annual exergoenvironmental impact rates due to irreversibility (B_i) were found to be associated with the combustion process, accounted for specifically in the combustion chamber and furnace heater. The main combustion components (air preheater, combustion chamber, and furnace heater) account for about 60% of the hybrid plant’s irreversibility-induced environmental impact rates. The reason for this is attributable to the high rate of exergy destruction in the combustion chamber and furnace heater, which are respectively the components with the first and third highest annual irreversibility rate in the hybrid plant. Next to the combustion equipment, the ORC unit also contributed significantly to the environmental impact rates of the hybrid plant, at about 38% of the total. It is worth noting here that, although the solar field has the second-highest rate of annual exergy destruction in the system, it has zero impact on the environment. This is because the solar system is fuelled exclusively by clean energy (solar irradiation), whose environmental impact rate is in itself null.

Regarding the environmental impact rate due to construction and pollutant emissions in system components (Y), results showed that the use of the solar system would only have a marginal effect on the annual impacts of the hybrid plant; less than 8% of the total. In addition, it can be deduced from the results in Table 5 that ORC components contributed the most in this case (about 72% of the total as against about 16% obtained for the combustion unit). Overall, the contribution of the ORC unit (about 52% of total) to the cumulative environmental impact rate (R) of the hybrid plant per year was estimated to be higher than that of the combustion unit (about 46% of total). The actual contribution of each system component to the cumulative environmental impact rate is illustrated in Fig. 4. The illustration reveals that the combustion chamber, furnace heater, ORC preheater, turbine, evaporator, and condenser have the highest relative total exergoenvironmental impacts. The implication is that, if careful attention is given to improving the exergoenvironmental performance of these components, the overall

Table 5
Exergoenvironmental impact rates for the hybrid plant components.

Component	b_f (Pts/MWh)	b_r (Pts/MWh)	E_f (MWh/year)	E_r (MWh/year)	E_i (MWh/year)	M (tons)	B_i (Pts/year)	Y (Pts/year)	R (Pts/year)
Solar field	0	3.8476	14954.8	1816.7	13138.1	1344.0	0	1278.3	1278.3
Hot tank	5.6491	5.8538	2842.70	2799.93	42.77	128.58	241.61	331.51	573.12
Cold tank	6.8856	7.2556	2098.42	2037.09	61.33	128.58	422.28	331.51	753.79
Air preheater	5.0583	29.734	245.42	42.79	202.62	1.20	1024.94	31.01	1055.95
Combustion chamber	2.1735	5.0583	25983.18	11665.20	14317.98	108.20	31119.64	2533.08	33652.72
Furnace heater	5.0583	7.2699	10800.82	7515.20	3285.63	0.0353	16619.84	0.07356	16619.91
ORC preheater	6.8856	10.6134	4738.83	3300.82	1438.01	93.0	9901.50	2403.49	12304.99
Evaporator	6.8856	11.2808	4482.60	3236.97	1245.63	218.0	8576.86	5650.47	14227.33
Recuperator	12.4283	17.6835	1990.23	1551.64	438.59	104.60	5450.89	2703.28	8154.17
Condenser	12.4283	64.4116	898.83	184.67	714.17	28.0	8875.90	723.63	9599.53
Pump	15.4558	35.6183	153.39	66.87	86.52	2.14	1337.24	8.73	1345.96
Turbine	12.4283	15.4558	5267.23	4255.19	1012.04	12.55	12577.97	302.31	12926.19
Valve 1	6.8856	6.8856	13702.87	13702.71	0.1556	0.56	-	-	-
Valve 2	6.8856	6.8856	4481.29	4475.12	6.17	0.56	-	-	-
System	2.1280	15.4558	40895.13	4101.80	36793.33	2169.96	96192.24	16299.69	112491.93

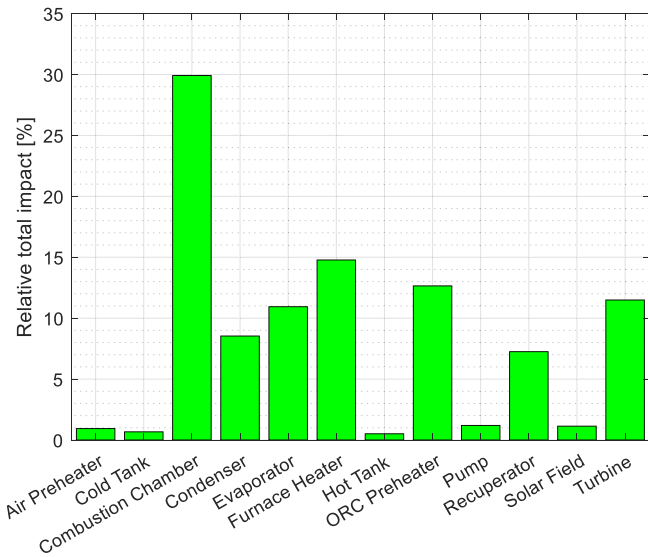


Fig. 4. Relative cumulative environmental impact rates of system components - hybrid solar-biomass plant.

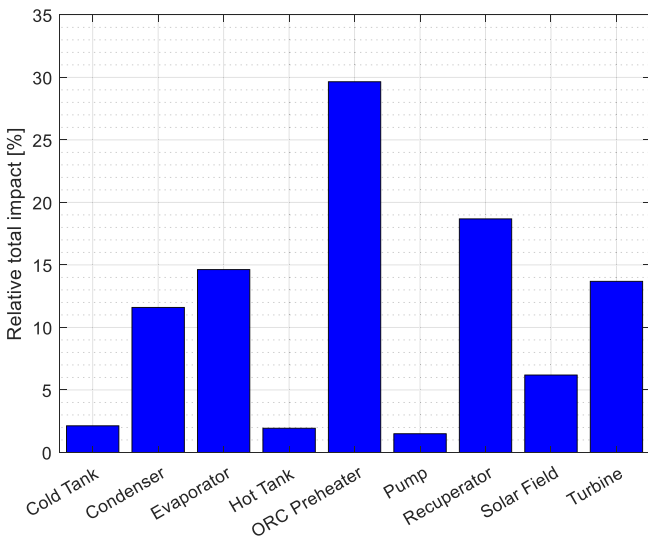


Fig. 5. Relative total environmental impacts of components – solar-only plant.

environmental impact of the hybrid plant would be significantly enhanced. Moreover, the measures required for the enhancement of the environmental performance of the plant should address not only the high rate of destroyed exergy in these components but also the inefficiencies in construction processes.

Furthermore, the exergoenvironmental performance of each system component is more explicitly highlighted using the established parameters reported in Table 6. The exergoenvironmental factor (f_b) weighs for each component the dominant cause of environmental impact rates. A high value of f_b signifies that environmental impact is predominantly due to construction processes and/or pollutant emissions; otherwise, the main cause is irreversibility in the respective components. Results showed that, although the cumulative impact rates are lower in the TES tanks compared to other components, the little impact they make on the environment is mainly due to the construction of these components. Amongst the components identified above with considerably high cumulative environmental impact rates, the ORC turbine, combustion chamber, air preheater, and ORC condenser attributed the annual impact rates mainly to thermodynamic irreversibilities. Additionally, other key results were inferred from the study using the relative difference of unit environmental impact rate (r_b) and specific environmental impact rate per unit energy (EIE) produced by the plant. High values of r_b signify that environmental impact rate of component product exergy contributes substantially to the effect, relative to the impact of the fuel exergy. In the case of EIE , the lower the value, the better the environmental performance of the system component. Since electrical power is the core product of the hybrid plant under study, the trend of EIE is analogous to that analyzed above for the cumulative environmental impact rate, with the highest impacts obtained in the ORC and combustion units. Particularly, the ORC unit contributes about 52% and the combustion unit about 46% to the total EIE obtained for the

Table 6
Exergoenvironmental performance parameters for the hybrid system components.

Component	f_b (%)	r_b (%)	EIE (Pts/MWh)
Solar field	100	-	0.3116
Hot tank	57.84	3.62	0.1397
Cold tank	43.98	5.37	0.1838
Air preheater	2.94	487.83	0.2574
Combustion chamber	7.53	132.73	8.2044
Furnace heater	0.0004	43.72	4.0519
ORC preheater	19.53	54.14	2.9999
Evaporator	39.72	63.83	3.4686
Recuperator	33.15	42.28	1.9879
Condenser	7.54	418.27	2.3403
Pump	0.65	130.45	0.3281
Turbine	2.36	24.36	3.1513
System	14.49	626.31	27.4250

hybrid plant. Generally, for the entire hybrid plant, the specific environmental impact per unit exergy of electrical energy was obtained to be 27.425 Pts/MWh.

Solar-only ORC plant

The exergoenvironmental impact results for the solar-only plant components are highlighted in Table 7. In this case, the highest annual exergoenvironmental impact rates due to irreversibility (B_I) were found to be associated with the ORC turbine, contributing about 37% to the total. However, the turbine has about the fourth largest annual exergy destruction rate next to the solar field, the preheater, and evaporator in descending order. Thus, the values of the specific exergoenvironmental indices of fuel play vital roles in the irreversibility-induced environmental impacts of the respective plant components. The environmental impact rates due to construction and pollutant emissions in the system components (Y) are the same for both the solar-only and hybrid plants. As can be seen in Table 7, the ORC preheater is presented with the largest annual cumulative environmental impact rate (R) of the solar-only plant, accounting for about 30% of the total. The actual contribution of each component to the cumulative environmental impact rate of the solar-only plant is self-revealing, as illustrated in Fig. 5.

Furthermore, the exergoenvironmental performance metrics are reported in Table 8 for the solar-only plant.

Exergoenvironmental comparison between the solar-only and hybrid solar-biomass plants

Furthermore, to allow for objective comparison of exergoenvironmental performance of the hybrid vs. the solar-only ORC plant, the main performance metrics adopted in this paper are juxtaposed in Figs. 6–8. As can be seen, the comparative exergoenvironmental analysis showed that introducing biomass section to the solar-ORC plant would impact negatively on the environment, as it would be expected. Particularly, the total exergoenvironmental impact rates per annum increased drastically with the introduction of biomass hybridization, by about 92,000 Pts/year, as seen in Fig. 6. The introduction of the biomass hybridization concept spikes exergoenvironmental impact rates in almost all the individual system components. This is obviously due to the nature of the biomass system considered in this study (biomass furnace with wood chips as combustion fuel); adopting other biomass system technologies/fuels could enhance the environmental effects of the hybrid scheme. Suffice to highlight here that irreversibilities in plant components dominate exergoenvironmental impact rates in the hybrid plant, while component construction activities dominate impact rates in the solar-only system. The foregoing statement is premised on values obtained for exergoenvironmental factors of the two systems, as illustrated in Fig. 7. Additionally, comparative analysis results show in Fig. 8 that annual environmental impact per unit exergy of 20.3 Pts/MWh was obtained for the solar-only ORC plant, as against the 27.4 Pts/MWh reported for the hybrid case. This amounts to about a 35% increase with biomass hybridization.

Table 7
Results of exergoenvironmental analysis of the solar-only ORC plant.

Component	b_F (Pts/MWh)	b_P (Pts/MWh)	E_I (MWh/year)	E_P (MWh/year)	E_T (MWh/year)	M (tons)	B_I (Pts/year)	Y (Pts/year)	R (Pts/year)
Solar field	0	1.3907	14954.75	2365.05	12589.70	1343.95	0	1278.26	1278.26
Hot tank	1.5839	1.6971	3576.24	3533.04	43.19	128.58	68.41	331.51	399.92
Cold tank	1.6971	1.8861	2389.13	2325.47	63.66	128.58	108.04	331.51	439.55
ORC preheater	1.6971	3.0103	1221.94	859.85	362.10	93.0	614.50	2403.49	3017.99
Evaporator	1.6971	9.7543	1034.97	759.34	275.63	218.0	467.76	5650.47	6118.23
Recuperator	10.1275	25.2258	514.16	400.45	113.71	104.60	1151.64	2703.28	3854.92
Condenser	10.1275	56.6758	216.36	51.43	164.93	28.0	1670.35	723.63	2393.98
Pump	12.7968	29.8406	41.55	18.11	23.44	2.14	299.93	8.73	308.65
Turbine	10.1275	12.7968	1307.22	1058.17	249.05	12.55	2522.29	302.31	2824.59
System	0	12.7968	14954.75	1016.62	13938.12	2,059.4	6902.91	13733.19	20636.09

Table 8
Exergoenvironmental performance parameters for the solar-only system components.

Component	f_b (%)	r_b (%)	EIE (Pts/MWh)
Solar field	100	–	1.2574
Hot tank	82.89	7.15	0.3934
Cold tank	75.42	11.14	0.4324
ORC preheater	79.64	77.38	2.9686
Evaporator	92.35	474.78	6.0182
Recuperator	70.13	149.08	3.7919
Condenser	30.23	459.62	2.3548
Pump	2.83	133.19	0.3036
Turbine	10.70	26.36	2.7784
System	66.55	Inf	20.2987

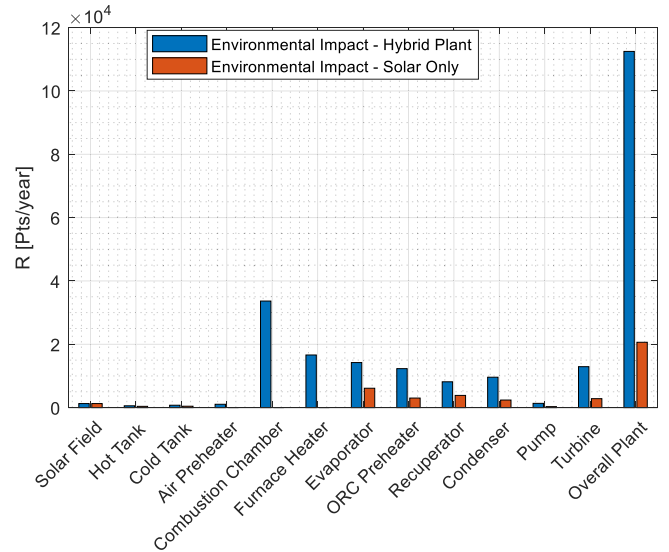


Fig. 6. Components and plant annual exergoenvironmental impact rates – hybrid vs. solar-only systems.

Conclusions

Annualized exergoenvironmental metrics were employed in this study to compare the performance of an ORC plant when powered by solar-only and hybrid solar-biomass heat sources. The ORC plant studied is based on a real 630 kW ORC system that currently runs solely on solar energy at Ottava, Italy. Due to the inconsistent availability of solar irradiation, the existing CSP-ORC plant is thermo-economically under-efficient. To optimize the system structurally, feasibility studies are ongoing to investigate the effects of parallel hybridization of a biomass heat source with the existing CSP system. Thus, a comparative analysis has been carried out in this paper, to investigate the potential effects that such hybridization concept would have on the environment from the Thermodynamics Second Law perspective. Particularly, the ORC plant

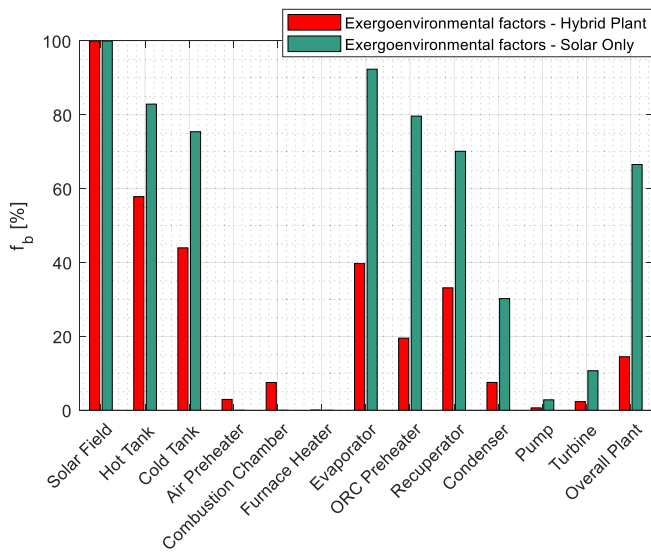


Fig. 7. Components and plant exergoenvironmental factors – hybrid vs. solar-only systems.

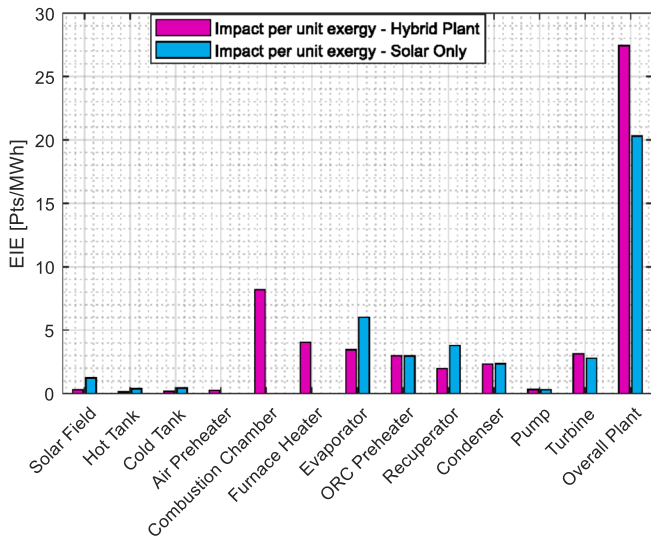


Fig. 8. Components and plant exergoenvironmental impact per unit produced work exergy – hybrid vs. solar-only systems.

was simulated in two case studies for one year, using established exergoenvironmental models. The same ORC design was adopted for each of the case studies; the first case used only the existing CSP system as the heat source, while the second assumed a hybrid CSP-biomass heat source. The main highlights of the study results are:

- Implementing the hybrid solar-biomass heat source would significantly improve annual exergy efficiency of the ORC plant, specifically by about 3 percentage points;

Appendix – Ecoindicator-99 Score Analysis for Plant Equipment

- The hybrid heat source would minimize effects of exergetic losses in the solar field on the overall system and enhance the plant capacity factor;
- The biomass hybridization concept would however equally increase the annual environmental impact per unit exergy from about 20 Pts/MWh obtained by the solar-only ORC plant to about 27 Pts/MWh, due to higher exergy destructions in the plant components and the polluting emissions of the combustor;
- Introducing a biomass section to the existing plant would as well worsen the specific exergoenvironmental impact per unit exergy produced by about 35%.

In sum, this study has shown clearly that using a hybrid solar-biomass system as a heat source for an ORC plant is capable of ameliorating some challenges common with solar-only ORC plants, such as low efficiencies, high energy losses, and low capacity factors. However, there is a somewhat high probability that implementing such a hybrid scheme would impact negatively the environment. To maximize the intended gain, there is, therefore, a need to carefully select the types of biomass technology and fuels to be integrated practically with solar systems to form hybrid plants. To the best of the authors’ knowledge, this paper is one of the first attempts to explicitly present annualized exergoenvironmental results for a hybrid solar-biomass ORC plant.

Further research can focus on the technological, economic, and environmental comparison of different biomass technology and fuel types for integration with the solar ORC plant. This would facilitate the analyses of the extent to which it could be possible to reduce environmental impact rates obtained in this study.

CRediT authorship contribution statement

Joseph Oyekale: Conceptualization, Methodology, Formal analysis, Investigation, Resources, Data curation, Writing – original draft, Writing – review & editing. **Mario Petrollese:** Methodology, Formal analysis, Investigation, Resources, Data curation, Writing – review & editing. **Daniele Cocco:** Conceptualization, Methodology, Investigation, Resources, Writing – review & editing, Visualization, Supervision. **Giorgio Cau:** Methodology, Investigation, Resources, Writing – review & editing, Visualization, Supervision, Project administration, Funding acquisition.

Declaration of Competing Interest

The authors declare that they have no known competing financial interests or personal relationships that could have appeared to influence the work reported in this paper.

Acknowledgments

This study was carried out under the Cooperation Agreement with “Ente Acque Sardegna” (ENAS) for the realization of the project “Thermodynamic solar plant for the development of an electrical and thermal energy smart grid” funded by P.O.R FESR 2014-2020 – Action line 4.3.1 – Framework agreement PT_CRP “Su Suercone Ambiente Identitario.”

The authors thank ENAS for providing operational data and information on the Ottana Solar Facility and for setting up the experimental ORC plant.

Component	Material	Composition (tons/%)	Eco'99 indicator (mpts/kg)	Component-based Eco'99 score (Y ^{CO} , mpts)	Operation-based Eco'99 score (Y ^{OP} , mpts/kg)	(Y ^{OP} , mpts)	Disposal Eco'99 score (Y ^{Cl} , mpts/kg)	(Y ^{Cl} , mpts)	Total Eco'99 score (pts)
Solar field	Aluminium	15.90/1.2%	420	6,678,000	7.9	10,617,205	- 69	-17,593,620	31,956.461
	Steel (piping)	5.02/0.4%	240	1,204,800					
	Stainless steel	4.12/0.3%	110	453,200					
	Glass (coated)	57.15/4.4%	51	2,914,650					
	Polystyrene (PS)	21.50/1.7%	370	7,955,000					
	Galvanized Steel	39.21/3.0%	86	3,372,060					
	Reinforcing steel	109.80 /4.2%	110	12,078,000					
	Rock wool (piping)	2.28/0.2%	61	139,080					
	Concrete	1088.97/84.5%	3.8	4,138,086					
	Sum	1343.95 ton		38,932,876					
TES (2 tanks)	Steel low alloy	-	110	-	16.9	4,346,004	-70	-18,001,200	16,575.464
	Foam glass	7.34/2.85%	58	425,720					
	Steel	32.5/12.6%	86	2,795,000					
	Rock wool	22.32/8.68%	61	1,361,520					
	Reinforcing steel	-	110	4,200,460					
	Cast iron	-	240	168,960					
	Copper	-	1400	1,974,000					
	Therminol SP-I (organic chemicals)	195 /75.8%	99	19,305,000					
Sum	257.16 tons		30,230,660						
Combustion chamber	Steel	36,074 kg/33.3%	86	3,102,364	20	2,164,000	-70	-7,574,000	63,327.024
	Steel high alloy	72126 kg/66.7%	910	65,634,660					
	Sum	108,200 kg		68,737,024					
Furnace heater	Steel low alloy	35.30 kg/100%	110	3,883	12.1	427	-70	-2471	1.839
Evaporator	Steel	54000 kg/24.8%	86	4,644,000	12.1	2,637,800	-70	-15,260,000	141,261.8
	Steel high alloy	164000 kg/75.2%	910	149,240,000					
	Sum	218,000 kg		153,884,000					
Pre-heater	Steel	23250 kg/25%	86	1,999,500	12.1	1,125,300	-70	-6,510,000	60,087.3
	Steel high alloy	69750 kg/75%	910	63,472,500					
	Sum	93,000 kg		65,472,000					
Recuperator	Steel	26150 kg/25%	86	2,248,900	12.1	1,265,660	-70	-7,322,000	67,582.06
	Steel high alloy	78450 kg/75%	910	71,389,500					
	Sum	104,600 kg		73,638,400					
Condenser	Steel	7000 kg/25%	86	602,000	12.1	338,800	-70	-1,960,000	18,090.8
	Steel high alloy	21000 kg/75%	910	19,110,000					
	Sum	28,000 kg		19,712,000					
Pump	Steel	760 kg/35.5%	86	65,360	16.9	36,166	-70	-149,800	218.126
	Aluminium	60 kg/2.8%	420	25,200					
	Steel low alloy	1200 kg/56.1%	110	132,000					
	Steel high alloy	120 kg/5.6%	910	109,910					
	Sum	2,140 kg		331,760					
Turbogenerator	Steel		86	326,800	11.7	146,835	-70	-878,500	7,557.635

(continued on next page)

(continued)

Component	Material	Composition (tons/%)	Eco'99 indicator (mpts/kg)	Component-based Eco'99 score (Y ^{CO} , mpts)	Operation-based Eco'99 score (Y ^{OP} , mpts/kg)	(Y ^{OP} , mpts)	Disposal Eco'99 score (Y ^{CL} , mpts/kg)	(Y ^{CL} , mpts)	Total Eco'99 score (pts)
	Steel high alloy	3800 kg/ 30.3%	910	7,962,500					
		8750 kg/ 69.7%							
	Sum	12,550 kg		8,289,300					
Valve 1	Steel low alloy	560 kg/100%	110	61,600	12.1	6,776	-70	-39,200	29.176
Valve 2	Steel low alloy	560 kg/100%	110	61,600	12.1	6,776	-70	-39,200	29.176
Air preheater	Steel	300 kg/25%	86	25,800	12.1	14,520	-70	-84,000	775.320
	Steel high alloy	900 kg/75%	910	819,000					
	Sum	1,200 kg		844,800					

References

[1] Danish, Ulucak R. A revisit to the relationship between financial development and energy consumption: is globalization paramount? *Energy* 2021;227:120337.

[2] World Energy Outlook 2019, 2019. doi:DOE/EIA-0383(2012) U.S.

[3] Pramanik S, Ravikrishna RV. A review of concentrated solar power hybrid technologies. *Appl Therm Eng* 2017;127:602–37. <https://doi.org/10.1016/J.APPLTHERMALENG.2017.08.038>.

[4] Middelhoff E, Andrade Furtado L, Peterseim JH, Madden B, Ximenes F, Florin N. Hybrid concentrated solar biomass (HCSB) plant for electricity generation in Australia: Design and evaluation of techno-economic and environmental performance. *Energy Convers Manag* 2021;240:114244.

[5] Tilahun FB, Bhandari R, Mamo M. Design optimization of a hybrid solar-biomass plant to sustainably supply energy to industry: methodology and case study. *Energy* 2021;220:119736. <https://doi.org/10.1016/j.energy.2020.119736>.

[6] Nami H, Anvari-Moghaddam A, Nemati A. Modeling and analysis of a solar boosted biomass-driven combined cooling, heating and power plant for domestic applications. *Sustain Energy Technol Assessments* 2021;47:101326. <https://doi.org/10.1016/j.seta.2021.101326>.

[7] Pina EA, Lozano MA, Serra LM, Hernández A, Lázaro A. Design and thermoeconomic analysis of a solar parabolic trough – ORC – biomass cooling plant for a commercial center. *Sol Energy* 2021;215:92–107. <https://doi.org/10.1016/j.solener.2020.11.080>.

[8] Meyer L, Tsatsaronis G, Buchgeister J, Schebek L. Exergoenvironmental analysis for evaluation of the environmental impact of energy conversion systems. *Energy* 2009;34:75–89. <https://doi.org/10.1016/j.energy.2008.07.018>.

[9] Cavalcanti EJC, Carvalho M, da Silva DRS. Energy, exergy and exergoenvironmental analyses of a sugarcane bagasse power cogeneration system. *Energy Convers Manag* 2020;222:113232. <https://doi.org/10.1016/j.enconman.2020.113232>.

[10] Mohammadi Hadelu L, Ahmadi Boyaghchi F. Exergoeconomic and exergoenvironmental analyses and optimization of different ejector based two stage expander-organic flash cycles fuelled by solar energy. *Energy Convers Manag* 2020;216:112943.

[11] Aghbashlo M, Tabatabaei M, Soltanian S, Ghanavati H. Biopower and biofertilizer production from organic municipal solid waste: an exergoenvironmental analysis. *Renew Energy* 2019;143:64–76. <https://doi.org/10.1016/j.renene.2019.04.109>.

[12] Wang W, Wang J, Lu Z, Wang S. Exergoeconomic and exergoenvironmental analysis of a combined heating and power system driven by geothermal source. *Energy Convers Manag* 2020;211:112765. <https://doi.org/10.1016/j.enconman.2020.112765>.

[13] Bonforte G, Buchgeister J, Manfrida G, Petela K. Exergoeconomic and exergoenvironmental analysis of an integrated solar gas turbine/combined cycle power plant. *Energy* 2018;156:352–9. <https://doi.org/10.1016/j.energy.2018.05.080>.

[14] Blumberg T, Lee YD, Morosuk T, Tsatsaronis G. Exergoenvironmental analysis of methanol production by steam reforming and autothermal reforming of natural gas. *Energy* 2019;181:1273–84. <https://doi.org/10.1016/j.energy.2019.05.171>.

[15] Fan G, Ahmadi A, Ehyaei MA, Das B. Energy, exergy, economic and exergoenvironmental analyses of polygeneration system integrated gas cycle, absorption chiller, and Copper-Chlorine thermochemical cycle to produce power, cooling, and hydrogen. *Energy* 2021;222:120008. <https://doi.org/10.1016/j.energy.2021.120008>.

[16] Ozbilen A, Dincer I, Rosen MA. Development of a four-step Cu-Cl cycle for hydrogen production - Part I: exergoeconomic and exergoenvironmental analyses. *Int J Hydrogen Energy* 2016;41:7814–25. <https://doi.org/10.1016/j.ijhydene.2015.12.184>.

[17] Boyano A, Blanco-Marigorta AM, Morosuk T, Tsatsaronis G. Exergoenvironmental analysis of a steam methane reforming process for hydrogen production. *Energy* 2011;36:2202–14. <https://doi.org/10.1016/j.energy.2010.05.020>.

[18] Razi F, Dincer I, Gabriel K. Exergoenvironmental analysis of the integrated copper-chlorine cycle for hydrogen production. *Energy* 2021;226:120426. <https://doi.org/10.1016/j.energy.2021.120426>.

[19] Parham K, Alimoradiyan H, Assadi M. Energy, exergy and environmental analysis of a novel combined system producing power, water and hydrogen. *Energy* 2017;134:882–92. <https://doi.org/10.1016/j.energy.2017.06.016>.

[20] Oyekale J, Heberle F, Petrollese M, Brüggemann D, Cau G. Biomass retrofit for existing solar organic Rankine cycle power plants: conceptual hybridization strategy and techno-economic assessment. *Energy Convers Manag* 2019;196:831–45. <https://doi.org/10.1016/j.enconman.2019.06.064>.

[21] Petrollese M, Oyekale J, Tola V, Cocco D. Optimal ORC configuration for the combined production of heat and power utilizing solar energy and biomass. *ECOS 2018 - Proc. 31st Int. Conf. Effic. Cost, Optim. Simul. Environ. Impact Energy Syst.* 2018.

[22] Oyekale J, Petrollese M, Cau G. Modified auxiliary exergy costing in advanced exergoeconomic analysis applied to a hybrid solar-biomass organic Rankine cycle plant. *Appl Energy* 2020;268:114888. <https://doi.org/10.1016/j.apenergy.2020.114888>.

[23] Mureddu M, Dessi F, Orsini A, Ferrara F, Pettinau A. Air- and oxygen-blown characterization of coal and biomass by thermogravimetric analysis. *Fuel* 2018;212:626–37. <https://doi.org/10.1016/j.fuel.2017.10.005>.

[24] Meteotest, Meteororm Software - Worldwide irradiation data, (n.d.).

[25] Cocco D, Migliari L, Petrollese M. A hybrid CSP-CPV system for improving the dispatchability of solar power plants. *Energy Convers Manag* 2016;114:312–23. <https://doi.org/10.1016/j.enconman.2016.02.015>.

[26] Petrollese M, Dickes R, Lemort V. Experimentally-validated models for the off-design simulation of a medium-size solar organic Rankine cycle unit. *Energy Convers Manag* 2020;224:113307.

[27] Environmental Management - Life Cycle Assessment - Requirements and Guidelines, I. 14044 International Organization for Standardization (ISO), (2006).

[28] Goedkoop M, Spriensma R. *The Eco-indicator 99 - a damage oriented method for Life Cycle. Impact Assessment* 2001.

[29] ecoinvent v3.7.1 – ecoinvent, (n.d.). <https://ecoinvent.org/the-ecoinvent-database/data-releases/ecoinvent-3-7-1/> (accessed January 11, 2022).

[30] Wernet G, Bauer C, Steubing B, Reinhard J, Moreno-Ruiz E, Weidema B. The ecoinvent database version 3 (part I): overview and methodology. *Int J Life Cycle Assess* 2016;21:1218–30. <https://doi.org/10.1007/s11367-016-1087-8>.

[31] Lazzaretto A, Tsatsaronis G. SPECO: A systematic and general methodology for calculating efficiencies and costs in thermal systems. *Energy* 2006;31:1257–89. <https://doi.org/10.1016/j.energy.2005.03.011>.

[32] Cavalcanti EJC, Carvalho M, Jonathan JL. Exergoenvironmental results of a eucalyptus biomass-fired power plant. *Energy* 2019;189:116188. <https://doi.org/10.1016/j.energy.2019.116188>.